DC Offset Performance of Four LMS Adaptive Algorithms

Abstract

The effects of DC offsets on four variations of the stochastic gradient algorithm are analyzed to determine the most appropriate algorithm for hardware implementation. The output mean squared error (MSE) performance in the presence of DC offsets is evaluated and compared with computer simulations for each of the algorithms assuming a Gaussian input distribution.

I. Introduction

The essence of an adaptive filter is the implementation of the algorithm that controls the filter coefficients. The four most common algorithms, which have been investigated extensively in the technical literature [1-5], in decreasing implementation complexity are: the least-mean-square (LMS) algorithm, the sign-data (SD-LMS), the sign-error (SE-LMS) and the sign-sign (SS-LMS) algorithms. It has been shown that all variants of the LMS algorithm converge only if the input signal is sufficiently exciting [4] and that even when sufficiency conditions are met, the SS-LMS and the SD-LMS algorithms can diverge due to gradient signal misalignment [4-6]. In addition, it has been shown that while both the LMS and the SD-LMS algorithms ideally achieve zero MSE, the SE-LMS and the SS-LMS algorithms experience finite minimum MSE [7] due to the fact that the step size for the coefficients does not go to zero.

When implementing *analog* adaptive filters, the effect of DC offsets is an important issue. Although some publications have treated DC offsets in adaptive filters [2], [8-11], few results are available on the effects of all sources of DC offsets on all four variations of the LMS algorithm. This paper investigates the performance of these algorithms from a DC offset point of view. To keep the analysis simple and tractable, discrete-time systems are analyzed and an adaptive linear combiner is studied. Simulation results are presented showing close agreement with the analytical work. Although this dc analysis is somewhat tedious, the results give insight as to the behavior of the algorithms as function of the unavoidable offset sources that would appear in any analog system. Specifically, the individual contribution of various offsets for a particular algorithm can be determined and reasons for the widely varying DC offset behaviours of the various algorthms are justified.

II. Problem Formulation

For an adaptive linear combiner, as shown in Fig. 1, the output at time index k is given by $\boldsymbol{y}_k = \boldsymbol{x}_k^T \boldsymbol{w}_k$ where $w_i(k)$ is the i^{th} coefficient value and $x_i(k)$ is the i^{th} gradient signal as well as the i^{th} input signal. The error signal is

$$e(k) = \delta(k) - y(k) = \boldsymbol{x}_k^T [\boldsymbol{w}^* - \boldsymbol{w}_k] \tag{1}$$

where $\delta(k)$ is the desired response and $\boldsymbol{w}^*$ is a vector of optimal coefficients. Defining $\boldsymbol{c}_k$ to be the present coefficient estimate, or mathematically

$$\boldsymbol{c}_k = \boldsymbol{w}^* - \boldsymbol{w}_k \tag{2}$$

then (1) can be re-written as

$$e(k) = \boldsymbol{x}_k^T \boldsymbol{c}_k \tag{3}$$

To allow a solution of otherwise very complicated expressions, it is also assumed that the gradient signals and the filter coefficient estimates are statistically independent, thus

$$E[\boldsymbol{x}_k^T \boldsymbol{c}_k] = E[\boldsymbol{x}_k^T] E[\boldsymbol{c}_k] \tag{4}$$

where E[•] represents the expectation operator. We also define $\sigma_x^2 \equiv E[x_i^2(k)]$ and $\sigma_e^2 \equiv E[e^2(k)]$

to be the mean-squared value of the gradient and the error signals, respectively. The quantity σ_e^2 represents the filter output MSE and is the performance measure to be evaluated.

The LMS algorithm, depicted in Fig. 2 for updating the ith coefficient, with modeled DC offsets inserted at appropriate locations using (2) is given by,

$$\text{LMS} \qquad \boldsymbol{c}_{k+1} = \boldsymbol{c}_k - 2\mu((\boldsymbol{x}_k + \boldsymbol{m}_{\mathbf{x}})(e(k) + m_e) + \boldsymbol{m}) \tag{5}$$

The vectors $\boldsymbol{m}_{\mathbf{x}}$ and $\boldsymbol{m}$ represent the unwanted DC offsets on each of the gradient signals and the equivalent DC offsets at the input of the accumulator (integrator) and at the output of the multiplier respectively. The term m_e represents the unwanted DC offset on the error signal and μ is a small step size that governs the adaptation rate. Similarly for the three other variants of the LMS algorithm we have:

$$\text{SD-LMS} \qquad \boldsymbol{c}_{k+1} = \boldsymbol{c}_k - 2\mu(\operatorname{sgn}[\boldsymbol{x}_k + \boldsymbol{m}_{\mathbf{x}}](e(k) + m_e) + \boldsymbol{m}) \tag{6}$$

$$\text{SE-LMS} \qquad \boldsymbol{c}_{k+1} = \boldsymbol{c}_k - 2\mu((\boldsymbol{x}_k + \boldsymbol{m}_{\mathbf{x}})\operatorname{sgn}[e(k) + m_e] + \boldsymbol{m}) \tag{7}$$

$$\text{SS-LMS} \qquad \boldsymbol{c}_{k+1} = \boldsymbol{c}_k - 2\mu(\operatorname{sgn}[\boldsymbol{x}_k + \boldsymbol{m}_{\mathbf{x}}]\operatorname{sgn}[e(k) + m_e] + \boldsymbol{m}) \tag{8}$$

III. The LMS Algorithm

Taking the expectation of both sides of (5) we obtain

$$E[\boldsymbol{c}_{k+1}] = E[\boldsymbol{c}_k] - 2\mu E[(\boldsymbol{x}_k + \boldsymbol{m}_{\mathbf{x}})(e(k) + m_e) + \boldsymbol{m}] \tag{9}$$

At steady-state (i.e. as $k \to \infty$), we have $E[\boldsymbol{c}_{k+1}] = E[\boldsymbol{c}_k]$. Using this fact together with (3-4), defining $\boldsymbol{R} \equiv E[\boldsymbol{x}_k \boldsymbol{x}_k^T]$ and dropping the time index k (for mathematical convenience), (9), for a zero-mean input distribution simplifies to

$$E[\boldsymbol{c}^T] = -(\boldsymbol{m} + m_e \boldsymbol{m}_{\mathbf{x}})^T \boldsymbol{R}^{-T} \tag{10}$$

To solve for the residual MSE due to offsets, we take the mean-squared value of both sides of (5)

$$E[\boldsymbol{c}_{k+1}^T \boldsymbol{c}_{k+1}] = E[\boldsymbol{c}_k^T \boldsymbol{c}_k] - 4\mu E[c_k^T((\boldsymbol{x}_k + \boldsymbol{m}_{\mathbf{x}})(e(k) + m_e) + \boldsymbol{m})]$$

$$+ 4\mu^2 E[((\boldsymbol{x}_k + \boldsymbol{m}_{\mathbf{x}})(e(k) + m_e) + \boldsymbol{m})^T((\boldsymbol{x}_k + \boldsymbol{m}_{\mathbf{x}})(e(k) + m_e) + \boldsymbol{m})] \tag{11}$$

Noting that at steady-state $E[\boldsymbol{c}_{k+1}^T \boldsymbol{c}_{k+1}] = E[\boldsymbol{c}_k^T \boldsymbol{c}_k]$, substituting (3) and (4) into (11) and dropping the time index as before, after some mathematical manipulation it can be shown that the approximation for small μ (by dropping μ^2 terms) governs the expression for the excess MSE at steady-state which is

$$\sigma_e^2 \approx (\boldsymbol{m} + m_e \boldsymbol{m}_{\mathbf{x}})^T \boldsymbol{R}^{-T} (\boldsymbol{m} + m_e \boldsymbol{m}_{\mathbf{x}}) . \tag{12}$$

The result in (12) shows that the excess MSE is inversely proportional to input signal power through the $\boldsymbol{R}^{-T}$ term and is directly sensitive to all offset sources. It should be noted that in analog implementations the DC offset at the output of the multiplier and at the input to the integrator, $\boldsymbol{m}$, would typically dominate.

IV. The Sign-Data LMS Algorithm

Taking the expectation of both sides of (6), using (3-4) and simplifying as before, for a zero-mean Gaussian noise input with variance $\sigma_x^2 = R_{ii}$ we have

$$E[\boldsymbol{c}^T] = -(\boldsymbol{m} + m_e \boldsymbol{k}_{\mathbf{mx}})^T \boldsymbol{R}_{\boldsymbol{MX}}^{-T} \tag{13}$$

where it can be shown from [12] and from Price's Theorem [13] respectively that

$$k_{mx_i} \equiv E[\mathrm{sgn}[x_i + m_{xi}]] = erf\left[\frac{m_{xi}}{\sqrt{2\sigma_x^2}}\right] \tag{14}$$

$$R_{mx_{i,j}} \equiv E[\mathrm{sgn}[x_i + m_{xi}] x_j^T] = \frac{1}{\sigma_x}\sqrt{\frac{2}{\pi}} e^{-m_{xi}^2/2\sigma_x^2} R_{i,j} \tag{15}$$

Taking the mean-squared value of both sides of (6) and simplifying as before yields

$$0 = \mu(N\sigma_e^2 + Nm_e^2 - \boldsymbol{m}^T\boldsymbol{m}) - E[\boldsymbol{c}^T](\boldsymbol{m} + m_e\boldsymbol{k}_{\mathbf{mx}}) - E[\boldsymbol{c}^T\mathrm{sgn}[\boldsymbol{x} + \boldsymbol{m}_{\mathbf{x}}]e] \tag{16}$$

Using (3) and (15), the last term in (16) for Gaussian white noise reduces to

$$E[\boldsymbol{c}^T\mathrm{sgn}[\boldsymbol{x} + \boldsymbol{m}_{\mathbf{x}}]\boldsymbol{x}^T\boldsymbol{c}] = \sqrt{\frac{2}{\pi}}\sigma_x\sum_{i=1}^{N}\hat{\sigma}_{c_i}^2 e^{-m_{xi}^2/2\sigma_x^2} \tag{17}$$

where $\hat{\sigma}_{c_i}^2 = \sigma_{c_i}^2 + E[c_i]^2$ and $\sigma_{c_i}^2$ represents the variance of c_i. Making use of the assumption in (4), for Gaussian white noise one can derive

$$\sigma_e^2 = \sigma_x^2\sum_{i=1}^{N}\hat{\sigma}_{c_i}^2 \tag{18}$$

Assuming that the mean-squared value of all the coefficient estimates are equivalent, or mathematically, $\hat{\sigma}_{c_i}^2 \approx \hat{\sigma}_{c_j}^2 \equiv \hat{\sigma}_c^2$ and that (17) and (18) are valid for colored Gaussian inputs, making use of (16-18) we obtain

$$\sigma_e^2 \approx \frac{\mu(Nm_e^2 - \boldsymbol{m}^T\boldsymbol{m}) + (\boldsymbol{m} + m_e\boldsymbol{k}_{\mathbf{mx}})^T\boldsymbol{R}_{\boldsymbol{MX}}^{-T}(\boldsymbol{m} + m_e\boldsymbol{k}_{\mathbf{mx}})}{\frac{1}{N\sigma_x}\sqrt{\frac{2}{\pi}}\sum_{i=1}^{N}e^{-m_{xi}^2/2\sigma_x^2} - \mu N} \tag{19}$$

The above assumptions are not true in general but as will be seen from the simulation results, their use yields satisfactory results. The expression in (19) shows that the performance of the SD-LMS algorithm is similar to the LMS algorithm from a DC offset point of view; the dominant offset terms appear explicitly in the numerator. The difference here is that the excess MSE is a weak function of the input signal power[1] for small μ. This effect is a consequence of the slicing operation which results in the loss of information as to signal amplitude and would be similarly manifested for arbitrary input distributions.

1. Signal power, σ_x^2, appears both in the numerator (via $\boldsymbol{R}_{\boldsymbol{MX}}^{-T}$) and denominator of (19).

V. The Sign-Error LMS Algorithm

Assuming $e(k)$ has a zero-mean Gaussian distribution at steady-state[2], taking the expectation of both sides of (7) and simplifying as before it can be shown that

$$E[\boldsymbol{c}^T] = -\sigma_e\sqrt{\frac{\pi}{2}}e^{m_e^2/2\sigma_e^2}\left(\boldsymbol{m} + erf\left[\frac{m_e}{\sqrt{2\sigma_e^2}}\right]\boldsymbol{m}_{\mathbf{x}}\right)^T\boldsymbol{R}^{-T} \tag{20}$$

Taking the mean-squared value of both sides of (7) and simplifying as before gives

$$0 = \mu(N\sigma_x^2 + \boldsymbol{m}_{\mathbf{x}}^T\boldsymbol{m}_{\mathbf{x}} - \boldsymbol{m}^T\boldsymbol{m}) - \sigma_e\sqrt{\frac{2}{\pi}}e^{-m_e^2/2\sigma_e^2} - E[\boldsymbol{c}^T]\boldsymbol{m} - E[\boldsymbol{c}^T\mathrm{sgn}[e + m_e]]\boldsymbol{m}_{\mathbf{x}} \tag{21}$$

Defining $\tilde{\boldsymbol{c}}^T$ to be a vector representing the AC component of the filter coefficient estimates, or mathematically, $\tilde{\boldsymbol{c}}^T \equiv \boldsymbol{c}^T - E[\boldsymbol{c}^T]$, and substituting into the last term in (21) yields

$$\begin{aligned}0 = {} & \mu(N\sigma_x^2 + \boldsymbol{m}_{\mathbf{x}}^T\boldsymbol{m}_{\mathbf{x}} - \boldsymbol{m}^T\boldsymbol{m}) - \sigma_e\sqrt{\frac{2}{\pi}}e^{-m_e^2/2\sigma_e^2} \\ & - E[\boldsymbol{c}^T]\left(\boldsymbol{m} + erf\left[\frac{m_e}{\sqrt{2\sigma_e^2}}\right]\boldsymbol{m}_{\mathbf{x}}\right) - E[\tilde{\boldsymbol{c}}^T\mathrm{sgn}[e + m_e]]\boldsymbol{m}_{\mathbf{x}}\end{aligned} \tag{22}$$

The last term in (22) measures the correlation of $\tilde{\boldsymbol{c}}^T$ with $\mathrm{sgn}[e + m_e]$ and is approximated to zero since for slow adaptation $\tilde{\boldsymbol{c}}^T$ is small. Thus, (22) with (20) provide a non-linear function in σ_e^2 that describes the MSE as function of μ and the interfering offsets. Although (22) is the main result for this section, it is also of interest to solve (22) for the limiting case of $\mu \to 0$:

2. This assumption becomes better for small μ for which the AC component of the coefficients is small and thus the distribution of the error signal follows that of the input.

$$\lim_{\mu \to 0} \sigma_e^2 = \frac{-m_e^2}{ln\left[\frac{\pi}{2}\left(\boldsymbol{m} + erf\left[\frac{m_e}{\sqrt{2\sigma_e^2}}\right]\boldsymbol{m}_{\mathbf{x}}\right)^T \boldsymbol{R}^{-T}\left(\boldsymbol{m} + erf\left[\frac{m_e}{\sqrt{2\sigma_e^2}}\right]\boldsymbol{m}_{\mathbf{x}}\right)\right]} \qquad (23)$$

Observe that the numerator of (23) consists of a typically smaller offset term (comparator input offset) than the denominator which consists of the dominant offset term $\boldsymbol{m}$. Thus in comparison with (12) or (19) one expects lower MSE for (23); especially when m_e is minimized which can be achieved using the technique in [14]. In fact, in the limiting case of $m_e = 0$ it can be shown that the MSE is shaped by μ and therefore achieves better MSE performance for small μ than (12) or (19). However it can also be shown from (22) that in the absence of DC offsets[3] the SE-LMS algorithm, unlike the LMS or the SD-LMS algorithm, will sustain a finite excess MSE that depends on μ.

It is also of interest to note that the degrading effects of DC offsets can be alleviated by passing the error signal through a high gain stage prior to coefficient computation [2]. This elegant solution is intuitively simple but is practically difficult to achieve in high-frequency applications. It is instructive to point out that the SE-LMS algorithm inherently provides this high gain and although non-linear is frequency independent.

VI. The Sign-Sign LMS Algorithm

Assuming $e(k)$ is Gaussian, taking the expectation of both sides of (8), making use of the work in [15] and the results of the previous sections, we have the following approximation[4]

$$E[\boldsymbol{c}^T] \approx -\sqrt{\frac{\pi}{2}}\sigma_e e^{m_e^2/2\sigma_e^2}\boldsymbol{m}^T\boldsymbol{R}_{MX}^{-T}. \qquad (24)$$

3. Not the case for analog circuits.
4. Although we cannot rigorously derive the result of (24) as yet, we believe the approximation models the actual result. The validity thereof, can be noted from the previous results and the simulations.

Taking the mean-squared value of both sides of (8) one obtains

$$0 = \mu(N - \boldsymbol{m}^T\boldsymbol{m}) - E[\boldsymbol{c}^T \mathrm{sgn}[\boldsymbol{x} + \boldsymbol{m}_{\mathbf{x}}]\,\mathrm{sgn}[e + m_e]] - E[\boldsymbol{c}^T]\boldsymbol{m} \tag{25}$$

Using [15], the procedure in obtaining (17-19), (24) and substituting (24) into (25) yields

$$0 \approx \mu(N - \boldsymbol{m}^T\boldsymbol{m}) - \frac{2}{\pi}\frac{\sigma_e}{\sigma_x}e^{-m_e^2/2\sigma_e^2}\frac{1}{N}\sum_{i=1}^{N} e^{-m_{xi}^2/2\sigma_x^2} + \sqrt{\frac{\pi}{2}}\sigma_e e^{m_e^2/2\sigma_e^2}\boldsymbol{m}^T\boldsymbol{R}_{MX}^{-T}\boldsymbol{m} \tag{26}$$

Again, a non-linear function in σ_e^2 is obtained that can be solved for the limiting case of small μ

$$\lim_{\mu \to 0} \sigma_e^2 \approx \frac{-m_e^2}{ln\left[\left(\frac{\pi}{2}\right)^{3/2}\sigma_x \frac{\boldsymbol{m}^T\boldsymbol{R}_{MX}^{-T}\boldsymbol{m}}{\frac{1}{N}\sum_{i=1}^{N} e^{-m_{xi}^2/2\sigma_x^2}}\right]} \tag{27}$$

The result shows that the SS-LMS algorithm in the presence of DC offsets has better excess MSE performance than the LMS algorithm or the SD-LMS algorithm for the same reasons elicited as for the SE-LMS algorithm. Notice in (27), as noted in (19), the predicted MSE is weakly dependent on the input signal power, σ_x^2. As well, it can be shown from (26) that for the case $m_e = 0$ or in the absence of DC offsets, the SS-LMS algorithm behaves like the SE-LMS algorithm.

VII. Numerical Verification

A 5-tap adaptive linear combiner configured as a model matching system was investigated to compare its simulated performance with the analytical predictions. A first-order lowpass filter was placed before the adaptive filter to allow the variation in signal statistics via α where

$$U(z) = \frac{1}{1 - \alpha z^{-1}} G(z) \tag{28}$$

The input distribution, $g(k)$, was Gaussian with zero mean and variance σ_x^2. The results of the simulations and the predicted analytical calculations are provided in Fig. 3. The bullets depict the predicted MSE calculated from equations (12), (19), (22) and (26) and the simulated MSE at the respective value for μ. A non-linear equation solver [16] was used to solve (22) and (26). The solid and dotted lines connect the bullets obtained from the analytical expressions and the simulations respectively to exemplify the behavior of the MSE as function of μ. The offset levels for the cases in Figs 3(a-c) are:

$$m_e = 0.01$$

$$\boldsymbol{m}_{\mathbf{x}}^T = \begin{bmatrix} 0.02 & -0.01 & -0.03 & -0.005 & 0.07 \end{bmatrix}$$

$$\boldsymbol{m}^T = \begin{bmatrix} 0.08 & 0.01 & -0.05 & -0.02 & -0.06 \end{bmatrix}$$

The offset levels for the case in Fig. 3d are:

$$m_e = 0.02$$

$$\boldsymbol{m}_{\mathbf{x}}^T = \begin{bmatrix} 0.02 & 0.0 & -0.07 & 0.05 & -0.008 \end{bmatrix}$$

$$\boldsymbol{m}^T = \begin{bmatrix} 0.03 & -0.1 & 0.005 & -0.08 & -0.06 \end{bmatrix}$$

Fig. 3a shows the case for a Gaussian white noise input. Figs. 3(b-d) show the results for more colored Gaussian inputs as given by the parameter α. Fig. 3c, unlike Figs. 3(a,b,d), shows the results when the input power is smaller than unity. Observe that in this case (compared with Fig. 3b) the excess MSE using the LMS algorithm is more sensitive to input power than either the SD-LMS or the SS-LMS algorithms as was predicted. For the case of Fig. 3d, the LMS algorithm showed evidence of divergence for the case $\mu = 0.01$ hence this point is omitted from the plot. The results of Fig. 3 verify the derived analytical expressions given by (12), (19), (22) and (26) for arbitrary offset levels and arbitrary input statistics. Specifically, note that the SE-LMS and the SS-

LMS algorithms are shaped by μ and that the limiting cases for $\mu \to 0$ expressed by (23) and (27) compare well with simulated data. Table 1 summarizes the results presented and the issues discussed in this paper.

Conclusions

We have analyzed and provided analytical expressions for the performance of four coefficient update algorithms for analog adaptive filters from an offset point of view. We have found that both the SE-LMS and the SS-LMS algorithms achieve better MSE performance when DC offsets are present; especially when integrator offsets, which dominate in a practical analog system, are unavoidable and in high frequency applications where simply passing the error signal through a gain stage to reduce the effects of DC offsets [2] is impractical. Having lower offset sensitivity, minimal circuit complexity combined with the fact that the SD-LMS and the SS-LMS algorithms can diverge due to gradient signal misalignment [5], we conclude that the SE-LMS algorithm is the best choice for practical high-frequency analog adaptive filters.

Acknowledgments

The authors appreciate Micronet's support for this work.

References

[1] J.R. Treichler, C.R. Johnson Jr. and M.G. Larimore, *Theory and Design of Adaptive Filters*, John Wiley & Sons Inc., New York, 1987.

[2] D.A. Johns, W. M. Snelgrove and A. S. Sedra, "Continuous-Time LMS Adaptive Recursive Filters," *IEEE Trans. Circuits Syst.*, vol. CAS-38, pp. 769-778, July 1991.

[3] H. Sari, "Performance Evaluation of Three Adaptive Equalization Algorithms," *IEEE Int. Conf. Acoust., Speech, Signal Processing*, vol. 3, pp. 1385-1389, May 1982.

[4] W.A. Sethares et al, "Excitation Conditions for Signed Regressor Least Mean Squares Adaptation," *IEEE Trans. Circuits Syst.*, vol. CAS-35, pp. 613-624, June 1988.

[5] T.A.C.M. Claasen and W.F.G. Mecklenbrauker, "Comparison of the Convergence of Two Algorithms for Adaptive FIR Digital Filters," *IEEE Trans. Acoust., Speech, Signal Processing*, vol. ASSP-29, pp. 670-678, June 1981.

[6] S. Dasgupta and C.R. Johnson Jr., "Some Comments on the Behavior of Sign-Sign Adaptive Identifiers," *Syst. Contr. Lett.*, vol. 7, April, 1986.

[7] C.R. Rohrs, C.R. Johnson and J.D. Mills, "A Stability Problem in Sign-Sign Adaptive Algorithms," *IEEE Int. Conf. Acoust., Speech, Signal Processing*, vol. 4, pp. 2999-3001, April 1986.

[8] T. Enomoto et al, "Integrated MOS Offset Error Canceller for Analogue Adaptive Transversal Filter," *Elect. Lett.*, vol. 19, pp. 968-970, Nov. 1983.

[9] U. Menzi and G.S. Moschytz, "Adaptive Switched Capacitor Filters Based on the LMS Algorithm," in *Proc. IEEE Int. Symp. Circuits and Systems*, vol. 3, pp. 2220-2223, May 1990.

[10] C.-P. J. Tzeng, "An Adaptive Offset Cancellation Technique for Adaptive Filters," *IEEE Trans. Acoust., Speech, Signal Processing*, vol. 38, pp. 799-803, May 1990.

[11] H. Qiuting, "Offset Compensation Scheme for Analogue LMS Adaptive FIR Filters," *Elect. Lett.*, vol. 28, pp. 1203-1205, June 1992.

[12] A. Papoulis, "*Probability, Random Variables, and Stochastic Processes*", Third Edition, McGraw-Hill, New York, 1991.

[13] R. Price, "A Useful Theorem for Nonlinear Devices Having Gaussian Inputs," *IRE Trans. Inform. Theory*, vol. IT-4, pp. 69-72, June 1958.

[14] A. Shoval, D.A. Johns and W.M. Snelgrove, "Median-Based Offset Cancellation Circuit Technique," in *Proc. IEEE Int. Symp. Circuits and Systems*, vol. 4, pp. 2033-2036, May 1990.

[15] H. Sari, *Algorithmes D'Egalisation Adaptive d'un Canal Dispersif*, Ph.D. thesis, Ecole Nationale Superieure des Telecommunications, Paris, October 1980.

[16] MATLAB, *Matrix Laboratory*, The MathWorks, Inc., Natwick MA, USA, 1992.

Table 1: Result Summary

<table>
<tr><th>Test Case</th><th>LMS</th><th>SD-LMS</th><th>SE-LMS</th><th>SS-LMS</th></tr>
<tr><td>input power</td><td>$\sigma_e^2 \propto 1/\sigma_x^2$</td><td>no effect</td><td>$\sigma_e^2 \propto 1/ln[\sigma_x^2]$</td><td>no effect</td></tr>
<tr><td>no offsets</td><td>$\sigma_e^2 \to 0$
for $\mu \to 0$</td><td>$\sigma_e^2 \to 0$
for $\mu \to 0$</td><td>$\sigma_e^2 \propto \mu^2 \sigma_x^4$</td><td>$\sigma_e^2 \propto \mu^2 \sigma_x^2$</td></tr>
<tr><td>all offsets</td><td colspan="2">σ_e^2 weakly depends on μ; for $\mu \to 0$
LMS
$\sigma_e^2 \propto (\boldsymbol{m} + m_e \boldsymbol{m}_{\mathbf{x}})^T (\boldsymbol{m} + m_e \boldsymbol{m}_{\mathbf{x}})$
SD-LMS
$\sigma_e^2 \propto (\boldsymbol{m} + m_e \boldsymbol{k}_{\mathbf{mx}})^T (\boldsymbol{m} + m_e \boldsymbol{k}_{\mathbf{mx}})$</td><td colspan="2">$\sigma_e^2$ strongly depends on μ; for $\mu \to 0$
SE-LMS
$\sigma_e^2 \propto \dfrac{m_e^2}{ln[(\boldsymbol{m} + \boldsymbol{m}_{\mathbf{x}})^T (\boldsymbol{m} + \boldsymbol{m}_{\mathbf{x}})]}$
SS-LMS
$\sigma_e^2 \propto \dfrac{m_e^2}{ln\left[\boldsymbol{m}^T \boldsymbol{m} / e^{m_{xi}^2/\sigma_x^2}\right]}$</td></tr>
<tr><td>$m_e = 0$</td><td>$\sigma_e^2 \propto \boldsymbol{m}^T \boldsymbol{m}$</td><td>$\sigma_e^2 \propto \boldsymbol{m}^T \boldsymbol{m}$</td><td colspan="2">$\sigma_e^2$ is scaled by μ^2
SE-LMS
$\sigma_e^2 \propto \mu^2 (\boldsymbol{m}^T \boldsymbol{m},\ \boldsymbol{m}_{\mathbf{x}}^T \boldsymbol{m}_{\mathbf{x}})^2$
SS-LMS
$\sigma_e^2 \propto \mu^2 \left(\boldsymbol{m}^T \boldsymbol{m},\ e^{m_{xi}^2/\sigma_x^2}\right)^2$</td></tr>
<tr><td>algorithm circuit complexity</td><td>1 multiplier/tap
1 integrator/tap</td><td>1 slicer/tap
1 trivial multi-plier/tap
1 integrator/tap</td><td>1 trivial multi-plier/tap
1 integrator/tap
1 slicer/filter</td><td>1 slicer/tap
1 XOR gate/tap
1 counter/tap
1 DAC/tap
1 slicer/filter</td></tr>
<tr><td>convergence</td><td>no gradient misalignment</td><td>gradients misaligned</td><td>no gradient misalignment</td><td>gradients misaligned</td></tr>
</table>

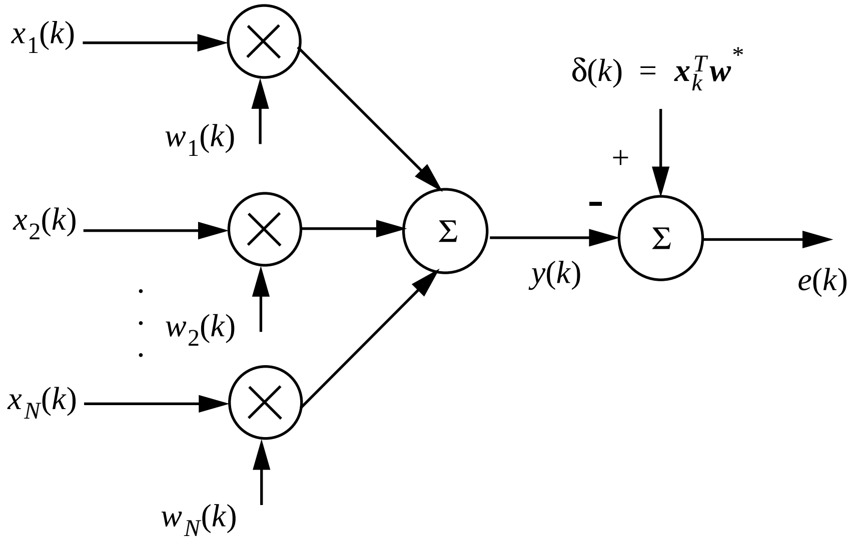

Fig. 1. A general adaptive linear combiner.

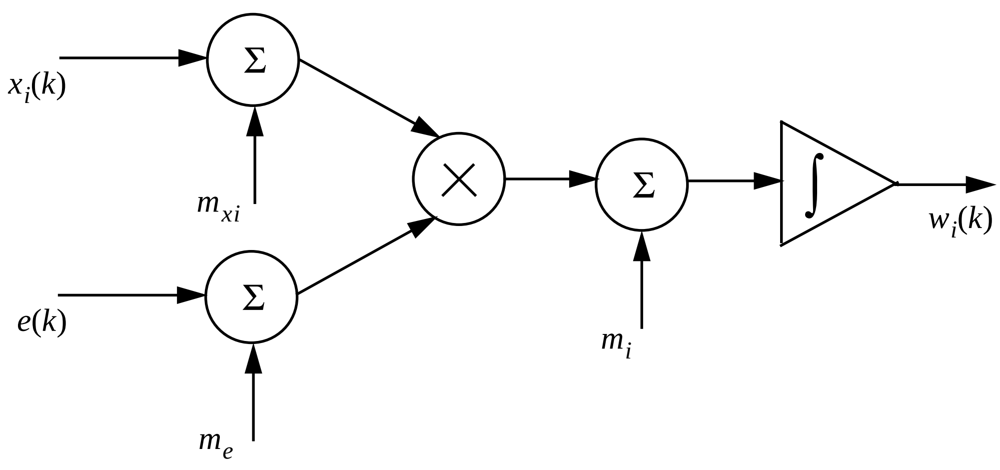

Fig. 2. Details of the LMS update circuitry showing DC offset sources.

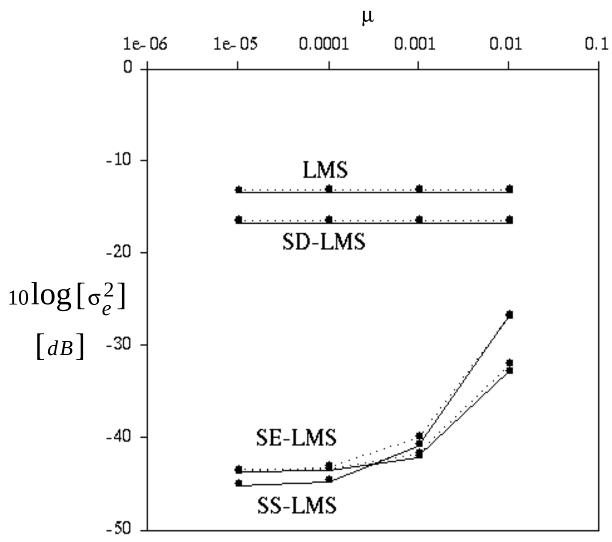

(a) $\alpha = 0, \ \sigma_x^2 = 1$

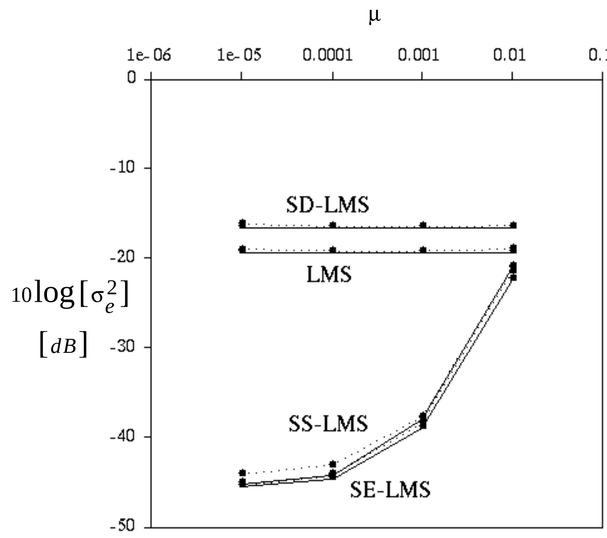

(b) $\alpha = 0.4, \ \sigma_x^2 = 1$

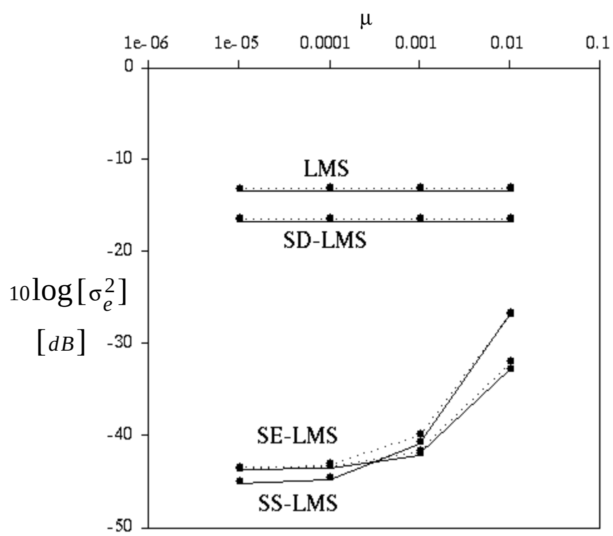

(c) $\alpha = 0.4, \ \sigma_x^2 = 0.25$

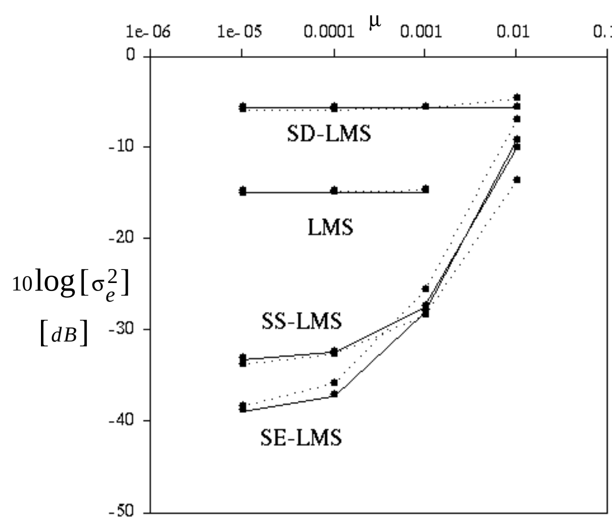

(a) $\alpha = 0.9, \ \sigma_x^2 = 1$

Fig. 3(a-d). Theoretical (dotted lines) and simulated (solid lines) MSE as function of μ, different offsets and different signal statistics for the four LMS based algorithms.